Editors' Suggestion | Featured in Physics

Emergence of Scale-Free Blackout Sizes in Power Grids

Tommaso Nesti,[1] Fiona Sloothaak,[2] and Bert Zwart[1,2]
[1]Centrum Wiskunde and Informatica, 1098 XG Amsterdam, Netherlands
[2]Eindhoven University of Technology, 5612 AZ Eindhoven, Netherlands

(Received 12 September 2019; revised 7 June 2020; accepted 10 July 2020; published 31 July 2020)

We model power grids as graphs with heavy-tailed sinks, which represent demand from cities, and study cascading failures on such graphs. Our analysis links the scale-free nature of blackout sizes to the scale-free nature of city sizes, contrasting previous studies suggesting that this nature is governed by self-organized criticality. Our results are based on a new mathematical framework combining the physics of power flow with rare event analysis for heavy-tailed distributions, and are validated using various synthetic networks and the German transmission grid.

DOI: 10.1103/PhysRevLett.125.058301

Securing a reliable power grid is of tremendous societal importance due to the highly disruptive repercussions of blackouts. Yet the study of cascading failures in power grids is a notoriously challenging problem due to its sheer size, combinatorial nature, mixed continuous and discrete processes, and physics and engineering specifications [1–5]. Traditional epidemics models [6–9] are unsuitable for its study, as the physics of power flow are responsible for a nonlocal propagation of failures [10]. This challenge has created extensive interest from the engineering and physics communities [11–17]. Analytic models determining the blackout size ignore the microscopic dynamics of power flow, while the analysis of more realistic networks typically does not go beyond simulation studies. Therefore, a fundamental understanding of blackouts is lacking.

The total blackout size, measured in terms of number of customers affected, is known to be *scale free* [18–21], meaning there exist constants C, $\alpha > 0$ such that

$$\mathbb{P}(S > x) \approx Cx^{-\alpha}, \tag{1}$$

where $\approx$ means that the ratio of both quantities approaches 1 as $x \to \infty$. This law, also known as the Pareto law, occurs in many applications of science and engineering [22–26]. Its significance in our context lies in the fact that big blackouts are substantially more likely than one would infer from more conventional statistical laws. As a result, mitigation policies cannot write off extremely large blackouts as virtually impossible events, and should focus on those in equal proportion to the small, frequent ones. Given the tremendous societal impact of large blackouts, understanding why Eq. (1) occurs can lead to focused prevention and/or mitigation policies and is therefore of major significance.

Several attempts to explain Eq. (1) have appeared in the literature. Using simulations, previous studies suggest that Eq. (1) may occur as a consequence of self-organized criticality [1,18,19,27,28]. Specifically, Ref. [18] compares simulation traces of a model for blackouts with those of a model that is known to exhibit self-organized criticality, and shows that the autocorrelation functions are similar. Such indirect analogies of different observables do not provide direct explanations into the precise mechanism behind Eq. (1).

Other strands of literature model the cascading mechanism as a branching process with critical offspring distribution [29], without taking physical laws of electricity into consideration. Such models lead to blackout sizes with infinite mean, corresponding to a value of $\alpha = 0.5$. While a naive parametric estimation procedure using all data would lead to values of α in the range (0,1), modern statistical techniques focusing on the tail end of the distribution clearly indicate a finite mean blackout size [20,21].

In this Letter, we propose a radically different and much simpler explanation than the aforementioned suggestions. Our central hypothesis is that Eq. (1) is inherited from a similar law for the distribution of *city sizes* [26,30–32]. We support this claim with a careful analysis of actual data, a new mathematical framework, and supporting simulations for additional insight and validation.

To develop intuition, we view the power grid as a connected graph where nodes represent cities, which are connected by edges modeling transmission lines. Initially, this is a single fully functioning network with balanced supply and demand. After several line failures, the network breaks into disconnected subnetworks, referred to as islands. The balance between supply and demand is not guaranteed to hold in each island, and at least one island is facing a power shortage. As the sum of total demand will be proportional to the total population in the island, the size of the power shortage is proportional to the total population, which is the sum of cities in that island. We now invoke a property of sums of Pareto distributed random variables, which informally says that the sum is dominated by the

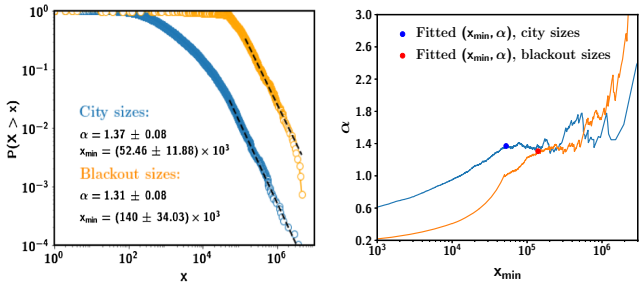

FIG. 1. Left: Pareto tail behavior of U.S. city [25] and blackout sizes [50] in the region $x > x_{\min}$. Estimates are based on PLFIT [25]. Points depict the empirical complementary cumulative distribution function (CCDF); solid line depicts the CCDF of a Pareto distribution with parameters $\alpha, x_{\min}$. Right: Hill estimator $x_{\min} \to \alpha(x_{\min})$, also known as the Hill plot [35]. The PLFIT estimates for city sizes (blue dot) and blackout sizes (red dot) lie within a relatively flat region of the graph, providing support for the Pareto fit.

maximum. In other words, the size of the largest city in this island drives the scale-free nature of the blackout. In extreme value theory, this is known as the principle of a single big jump [33,34].

This line of reasoning implies that city sizes and blackout sizes both have Pareto distributions with similar tail behavior. For the case of the U.S. blackout sizes (in terms of the number of customers affected) and city sizes (in terms of population), we confirm this with historical data as summarized in Fig. 1, which shows that the parameters α for blackout and city sizes distributions are remarkably similar, each having a finite mean. See Supplemental Material [35], Sec. II, for details.

In what follows, we make our claim rigorous by introducing a new mathematical framework that captures the salient characteristics of actual power system dynamics [1] and sheds light on the connection between blackout and city sizes. For a full account, see Ref. [35], Sec. IV.

We consider a network with n nodes and m lines. Node i represents a city with X_i inhabitants. We consider a static setting where each inhabitant demands one unit of energy. We assume that the X_i's are independent and identically distributed Pareto random variables with $\mathbb{P}(X > x) \approx Kx^{-\alpha}$ for constants $K, \alpha > 0$. For convenience, we label the nodes such that X_1 represents the largest city.

For the electricity line flows, we adopt a linear dc power flow model. This model approximates the more involved ac power flow equations, is widely used in high-voltage transmission system analysis [51], and accurately described the evolution of the 2011 San Diego blackout [52]. Specifically, if $\mathbf{g} = (g_1, \ldots, g_n)$ and $\mathbf{X} = (X_1, \ldots, X_n)$ represent the power generation and demand at each city, then the line flows $\mathbf{f} = (f_1, \ldots, f_m)$ are given by $\mathbf{f} = \mathbf{V}(\mathbf{g} - \mathbf{X})$, where the matrix $\mathbf{V} \in \mathbb{R}^{m \times n}$ is determined by the network topology and the line reactances.

Our framework consists of three stages called planning, operational, and emergency. The first two stages determine the actual line limits and line flows. We employ the widely used direct current optimal power flow (dc OPF) formulation with quadratic supply cost functions [1]:

$$\min_{\mathbf{g}} \frac{1}{2} \sum_{i=1}^{n} g_i^2$$
$$\text{such that } \sum_{i=1}^{n} g_i = \sum_{i=1}^{n} X_i, \tag{2}$$

subject to the reliability constraint

$$-\bar{\mathbf{f}} \le \mathbf{V}(\mathbf{g} - \mathbf{X}) \le \bar{\mathbf{f}}. \tag{3}$$

The planning stage concerns how the operational line limits $\bar{\mathbf{f}}$ are set. For this, we solve Eq. (2) without Eq. (3), yielding the uniform (across cities) solution $g_j^{(\mathrm{pl})} = (1/n) \sum_{i=1}^{n} X_i$ for all $j \ge 1$, and $\mathbf{f}^{(\mathrm{pl})} = -\mathbf{V}\mathbf{X}$ (see Ref. [35], Sec. IV). Then, the operational line limits $\bar{\mathbf{f}}$ are set as

$$\bar{f}_\ell = \lambda |f_\ell^{(\mathrm{pl})}| = \lambda |(\mathbf{V}\mathbf{X})_\ell|, \qquad \ell = 1, \ldots, m, \tag{4}$$

where $\lambda \in (0, 1]$ is a safety tuning parameter, referred to as loading factor. In the operational stage, we solve Eq. (2) subject to Eq. (3), yielding a different solution $\mathbf{g}^{(\mathrm{op})}$ which is not uniform due to the constraint (3). Equation (4) implies that line flows can have a heavy tail, which is consistent with impedance data [53]. This property is essential, as it allows us to create a subnetwork in which the mismatch between supply and demand is heavy tailed.

This mismatch is established in the emergency stage, which is described next. We focus on cascades initiated by a single line failure, sampled uniformly across all lines. A line failure changes the topology of the grid and causes a global redistribution of network flows according to power flow physics. Consecutive failures occur whenever there are one or more lines for which the redistributed power flow exceeds its emergency line limit $F_\ell = \bar{f}_\ell / \lambda$. Failures are assumed to occur subsequently, and take place at the line where the relative exceedance is largest. Whenever line failures create additional islands, we proportionally lower either generation or demand at all nodes to restore power balance. The cascade continues within each island until none of the remaining emergency line limits are exceeded anymore.

Our formulation may be extended to handle multiple initial failures, correlated city sizes, generator failures, simultaneous failures, generation limits, other strictly convex supply cost functions, and other load-shedding mechanisms. Such variations would affect the value of the prefactor C, but not the exponent α: the tail of the blackout distribution is dominated by the scenario where there is a single city that has a large power demand, while the demand of the other cities is negligible. A formal version of this statement is that, for sufficiently small ϵ,

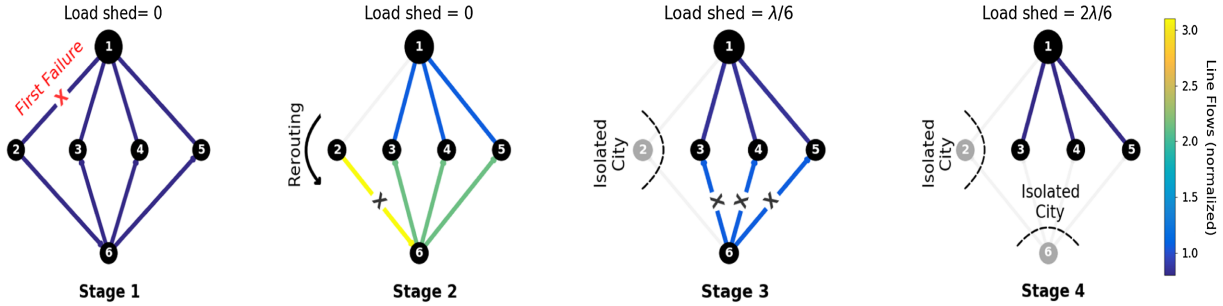

FIG. 2. Cascade in a six-node network with $X_1 = 1$, $X_j = 0$ for $j \geq 2$, $\lambda > 3/4$. The four lower and upper line flows are $\lambda/24$ and $5\lambda/24$, respectively, with corresponding emergency limits $1/24$ and $5/24$. The failure of an upper line causes the load on the adjacent lower line to surge to $\lambda/6 > 1/24$, causing this line to trip (stage 2). This cutoff leads to the load on the three remaining lower lines to surge to $\lambda/18$, causing them to trip as well (stage 3). After isolating nodes 2 and 6, the cascade ends with $|A_1| = 4$ and a total load shed of $2\lambda/6$ (stage 4).

$$\mathbb{P}(S > x) = \mathbb{P}(S > x; X_1 > x, X_i \leq \epsilon x, i \geq 2) + o(x^{-\alpha}). \tag{5}$$

This is a mathematical description of the aforementioned principle of a single big jump. After a normalization argument, it suffices to consider the case where $X_1 = y > 0$ and $X_j = 0$ for $j \geq 2$. Then, the solution of the operational dc OPF can be computed in closed form: $g_1^{(\mathrm{op})} = [1 - \lambda(n-1)/n]y$ and $g_j^{(\mathrm{op})} = (\lambda/n)y$ for $j \geq 2$ (see Ref. [35], Lemma 4.2). Let A_1 be the set of nodes that represents the island containing the largest city, after the cascade has stopped. The islands that do not contain the largest city must lower their generation to zero after a disconnection, and hence immediately turn stable. Iterating, the blackout size in component A_1 is given by

$$S = \sum_{i \in A_1} (X_i - g_i) = \sum_{j \notin A_1} (g_j - X_j) = \lambda \frac{n - |A_1|}{n} y. \tag{6}$$

Integrating over realizations of $X_1 = y$, $y \geq x$, and using the property of Pareto tails $\mathbb{P}(\max(X_1, \ldots, X_n) > x) \approx n\mathbb{P}(X > x) \approx nKx^{-\alpha}$ [33], we find that Eq. (1) holds with

$$C = nK \sum_{j=1}^{n-1} \mathbb{P}(|A_1| = j)\lambda^{\alpha}(1 - j/n)^{\alpha} \in [0, \infty). \tag{7}$$

The most delicate step, for which Ref. [35], Sec. IV.D provides a rigorous proof, is to show that the cascade sequence does not change when performing the normalization argument in the limit $x \to \infty$, which is nontrivial due to continuity issues.

In Ref. [35], Sec. IV, we show that the prefactor C in Eq. (7) is discontinuous at a discrete set of values of λ. At such points, the number of possible scenarios leading to a large blackout is increasing and/or $|A_1|$ is decreasing in λ. We illustrate this in Fig. 2, which also shows how the principle of a single big jump (5), which links the total blackout size to the size of the largest city X_1, is realized by means of a few load-shedding events, each of which is a fixed fraction of X_1 and corresponds to a network disconnection.

Our analysis illustrates how heavy-tailed city sizes cause heavy-tailed blackout sizes. Our modeling choices allow for a precise exploration of the cascade sequence, and, inherently, an explicit formula for the blackout size tail. However, we emphasize that the essential elements that lead to heavy-tailed blackout sizes are that both the demands and the line limits are heavy tailed. The small nodes together generate a non-negligible fraction of the demand of the large node. When the power grid satisfies these properties, then Eq. (5) continues to hold, leading to a heavy-tailed mismatch whenever there is a disconnection. We illustrate this numerically by studying the effect of relaxing several assumptions in our framework.

The choice of a quadratic cost function in the dc OPF ensures that it is most efficient to divide the power generation as equally as possible among the cities, causing all cities to generate a non-negligible fraction of the total demand. Other strictly convex increasing cost functions would lead to a similar effect. Moreover, our result is robust to piecewise linear cost functions (see Ref. [35], Sec. VI.C), and to the inclusion of generation limits, as long as these limits are a non-negligible fraction of the total demand.

To illustrate the sensitivity of our result with respect to the chosen power flow model, we partially extend our framework to the ac power flow model. We tested its effect on multiple network topologies, and as illustrated in Fig. 3(a), we conclude that city size tails still drive the blackout size tail even when the dc assumption is violated. Intuitively, the chosen power flow model determines the redistribution of flow after failures, and thus the cascade sequence. This effect is captured in the prefactor, but does not destroy the Pareto-tailed consequence in the blackout size.

An important remark is that our mathematical framework relies on the city sizes to be random variables. Naturally, city sizes are essentially fixed. The remaining source of

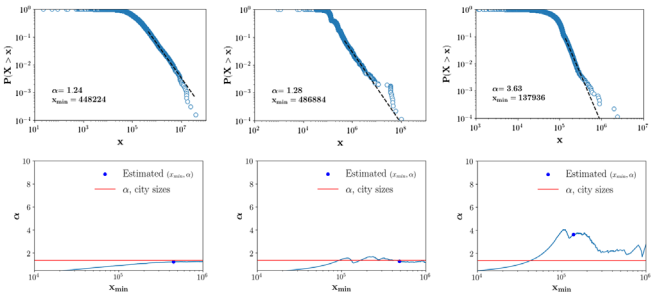

(a) IEEE 39-bus network, ac power flow model.

(b) SynGrid model, $n = 10^4$, frozen city sizes.

(c) SynGrid model, $n = 10^4$, frozen city sizes sampled from uniform distribution.

FIG. 3. Pareto tail behavior of simulated blackout sizes using the described cascade model with relaxed assumptions, for different topologies and loading factor $\lambda = 0.9$. City sizes are sampled from a Pareto distribution with tail index $\alpha^{(\mathrm{city})} = 1.37$ in (a),(b), and from a uniform distribution with the same mean in (c). Top: Points depict the empirical CCDF, dashed line depicts the CCDF of a Pareto distribution with parameters α, $x_{\min}$, estimated via PLFIT [25]. Bottom: Hill plots. Red line corresponds to the tail index $\alpha^{(\mathrm{city})}$. A good fit is achieved when the PLFIT estimate (blue dot) lies in a flat region closely tracing the red line.

randomness in our framework, namely the location of the first failure, can be interpreted as a mechanism to bootstrap linear combinations of city sizes. It is well known [33] that bootstrap methods cannot recover heavy-tailed behavior if the dataset is small. In order to recover a Pareto tail, the frozen network therefore needs to be sufficiently large, e.g., 10^4 nodes. To illustrate this, Fig. 3(b) shows simulation results for the SynGrid model, a random graph model designed to generate realistic power grid topologies [53]. Finally, Fig. 3(c) reveals that Pareto-tailed city sizes is a crucial assumption in order to recover the same scale-free behavior for blackout sizes, as light-tailed city sizes do not lead to heavy-tailed blackout sizes. Additional supporting experiments are reported in Ref. [35], Sec. VI.

We next present experimental results using the SciGRID network [54,55], a model of the German transmission grid that includes generation limits and relaxes several assumptions. We simulate blackout realizations by considering one year's worth of hourly snapshots. For each snapshot, we solve the operational dc OPF and remove one line uniformly at random, initiating a cascade. To assign city sizes to nodes, we have cities correspond to German districts, and we assign a fraction of the population of each district to specific nodes based on a Voronoi tessellation procedure. In this way, we account for the feature that a single city can encompass multiple nodes in a network. For more details, see Ref. [35], Sec. VII.

The German SciGRID network has a relatively small number of nodes (less than 600), and city sizes are frozen. Therefore, we do not recover Pareto-tailed blackout sizes. However, uniformly across different loading factors λ, we found that the preponderance of blackouts involves just a single load-shedding event due to a network disconnection. For a moderate loading factor $\lambda = 0.7$, nearly 98% of blackouts only involve a single disconnection. Even for a high loading factor $\lambda = 0.9$, 90% of the blackouts involve a single disconnection, and the fraction of blackouts with four or more disconnections is below 4%. Figure 4 depicts the largest observed blackout, for different values of λ. Even in these massive blackouts, the bulk of the total load shed is the result of a few load-shedding events. These observations are typical properties that follow from our framework (see Fig. 2), and sharply contrast the branching process approximations where many small jumps take place.

Using data analysis, probabilistic analysis, and simulations, we have illustrated how extreme variations in city sizes can cause the scale-free nature of blackouts. Our explanation and refinement (7) of the scaling law (1) show that specific details such as network characteristics only appear in the prefactor (7). The main parameter α, which determines how fast the probability of a big blackout vanishes as its size grows, is completely determined by the city size distribution. Decreasing the constant (7) by performing network upgrades (which in our framework is equivalent to decreasing λ) would only lead to a modest decrease in the likelihood of big blackouts. Consequently, it is questionable whether network upgrades, as considered in Refs. [19,56], are the most effective way to mitigate the consequences of big blackouts.

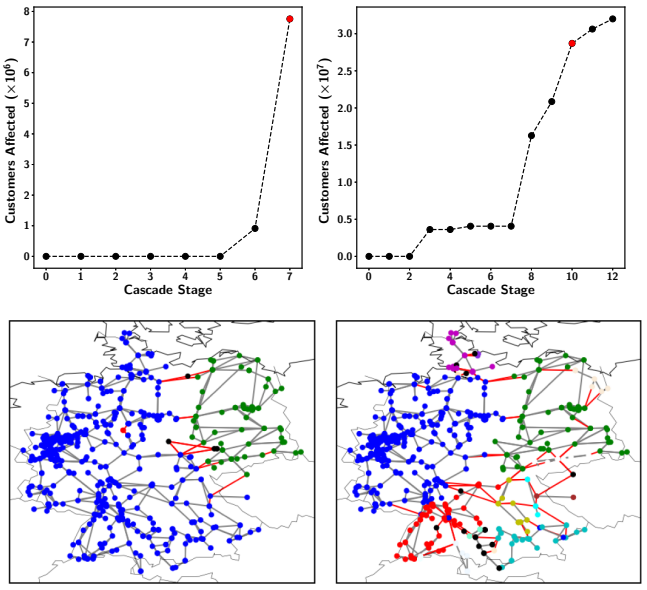

FIG. 4. Dissection of a massive blackout in the SciGRID network for loading factors $\lambda = 0.7$ (left) and $\lambda = 0.9$ (right) in terms of the cumulative number of affected customers at each stage of the cascade, as displayed in the top charts with the selected stage colored red. The corresponding islanded components are visualized with different colors in the bottom illustrations.

Instead, it may be more effective to invest in responsive measures that enable consumers to react to big blackouts. It is shown in Ref. [20] that durations of blackouts have a tail which is decreasing much faster than Eq. (1). At the same time, production facilities often lack redundancy—even short blackouts can lead to huge costs, suggesting that the costs associated to a blackout are concave up to a certain duration. Therefore, if the goal is to minimize the negative effects of a big blackout, it may be far more effective to invest in solutions (such as local generation and storage) that aim at surviving a blackout of a specific duration. This is consistent with recent studies on the importance of resilient city design [57].

Finally, our framework and insights suggest new ways of approaching scale-free phenomena in other transportation networks, such as highway traffic jams [58]. While transport network topologies are not scale free, they may still exhibit scale-free behavior, caused by the scale-free nature of nodal sizes.

We thank Sem Borst for useful discussions, and the Isaac Newton Institute for support and hospitality during the program "Mathematics of Energy Systems." Financial support was received from Grants No. NWO 639.033.413, No. NWO 024.002.003, and EPSRC No. EP/R014604/1.

[1] D. Bienstock, *Electrical Transmission System Cascades and Vulnerability—An Operations Research Viewpoint*, MOS-SIAM Series on Optimization Vol. 22 (SIAM, Philadelphia, 2016).
[2] F. Dörfler, M. Chertkov, and F. Bullo, Proc. Natl. Acad. Sci. U.S.A. **110**, 2005 (2013).
[3] J. W. Simpson-Porco, F. Dörfler, and F. Bullo, Nat. Commun. **7**, 10790 (2016).
[4] B. Schäfer, D. Witthaut, M. Timme, and V. Latora, Nat. Commun. **9**, 1975 (2018).
[5] T. Nesti, A. Zocca, and B. Zwart, Phys. Rev. Lett. **120**, 258301 (2018).
[6] D. Watts, Proc. Natl. Acad. Sci. U.S.A. **99**, 5766 (2002).
[7] F. Morone and H. A. Makse, Nature (London) **524**, 65 (2015).
[8] J. Hindes and I. B. Schwartz, Phys. Rev. Lett. **117**, 028302 (2016).
[9] R. Pastor-Satorras and A. Vespignani, Phys. Rev. Lett. **86**, 3200 (2001).
[10] P. D. H. Hines, I. Dobson, and P. Rezaei, IEEE Transactions on Power Systems **32**, 958 (2017).
[11] A. E. Motter, Phys. Rev. Lett. **93**, 098701 (2004).
[12] D. Witthaut, M. Rohden, X. Zhang, S. Hallerberg, and M. Timme, Phys. Rev. Lett. **116**, 138701 (2016).
[13] Y. Yang and A. E. Motter, Phys. Rev. Lett. **119**, 248302 (2017).
[14] B. Schäfer, C. Beck, K. Aihara, D. Witthaut, and M. Timme, Nat. Energy **3**, 119 (2018).
[15] D. Witthaut and M. Timme, Phys. Rev. E **92**, 032809 (2015).
[16] P. Crucitti, V. Latora, and M. Marchiori, Phys. Rev. E **69**, 045104(R) (2004).
[17] L. Huang, L. Yang, and K. Yang, Phys. Rev. E **73**, 036102 (2006).
[18] B. A. Carreras, V. E. Lynch, I. Dobson, and D. E. Newman, Chaos **14**, 643 (2004).
[19] I. Dobson, B. A. Carreras, V. E. Lynch, and D. E. Newman, Chaos **17**, 026103 (2007).
[20] P. Hines, K. Balasubramaniam, and E. C. Sanchez, IEEE Potentials **28**, 24 (2009).
[21] B. A. Carreras, D. E. Newman, and I. Dobson, IEEE Transactions on Power Systems;IEEE Transactions on Power Electronics **31**, 4406 (2016).
[22] A.-L. Barabási and R. Albert, Science **286**, 509 (1999).
[23] B. Suki, A.-L. Barabási, Z. Hantos, F. Peták, and H. E. Stanley, Nature (London) **368**, 615 (1994).
[24] A.-L. Barabási, Nature (London) **435**, 207 (2005).
[25] A. Clauset, C. R. Shalizi, and M. E. Newman, SIAM Rev. **51**, 661 (2009).
[26] H. A. Simon, Biometrika **42**, 425 (1955).
[27] P. Bak, C. Tang, and K. Wiesenfeld, Phys. Rev. A **38**, 364 (1988).
[28] K. Sun, Y. Hou, W. Sun, and J. Qi, *Power System Control Under Cascading Failures: Understanding, Mitigation, and System Restoration* (Wiley-Blackwell, New York, 2018).
[29] J. Kim and I. Dobson, IEEE Trans. Reliabi. **59**, 691 (2010).
[30] G. K. Zipf, Soc. Forces **28**, 340 (1950).
[31] K. T. Rosen and M. Resnick, J. Urban Econ. **8**, 165 (1980).
[32] M. Batty, Science **319**, 769 (2008).
[33] S. I. Resnick, *Heavy-Tail Phenomena, Springer Series* in Operations Research and Financial Engineering (Springer, New York, 2007). pp. XIX–404.
[34] J. Nair, A. Wierman, and B. Zwart, Eval. Rev. **41**, 387 (2013).
[35] See Supplemental Material at http://link.aps.org/supplemental/10.1103/PhysRevLett.125.058301 for the extended mathematical framework and the details on the statistical data analysis and simulations, which includes Refs. [36–49].
[36] B. M. Hill, Ann. Stat. **3**, 1163 (1975).
[37] P. v. Mieghem, *Graph Spectra for Complex Networks* (Cambridge University Press, Cambridge, England, 2010).
[38] P. Van Mieghem, K. Devriendt, and H. Cetinay, Phys. Rev. E **96**, 032311 (2017).
[39] P. TøNdel, T. A. Johansen, and A. Bemporad, Automatica **39**, 489 (2003).
[40] D. J. Watts and S. H. Strogatz, Nature (London) **393**, 440 (1998).
[41] Z. Wang, H. Sadeghian, S. H. Elyas, R. D. Zimmerman, E. Schweitzer, and A. Scaglione, SynGrid User's Manual (2019), https://matpower.org/docs/SynGrid-manual.pdf.
[42] R. D. Zimmerman, C. E. Murillo-Sánchez, and R. J. Thomas, IEEE Trans. Power Syst. **26**, 12 (2011).
[43] D. K. Molzahn and I. A. Hiskens, *A Survey of Relaxations and Approximations of the Power Flow Equations* (2019), Vol. 4, pp. 1–221.
[44] T. Brown, https://pypsa.org/examples/scigrid-lopf-then-pf.html.
[45] World Population Review, http://worldpopulationreview.com/countries/germany-population/cities/, accessed Oct. 2018.

[46] Eurostat, http://appsso.eurostat.ec.europa.eu/nui/show.do?dataset=nama_10r_3popgdp, accessed Oct. 2018.
[47] Eurostat, Nuts_rg_60m_2013.shp, https://ec.europa.eu/eurostat/web/gisco/geodata/reference-data/administrative-units-statistical-units/nuts#nuts13, accessed Oct. 2018.
[48] Data Packaged Core Datasets, Nuts_rg_60m_2013.shp, https://github.com/datasets/geo-nuts-administrative-boundaries/blob/master/data/NUTS_2013_60M_SH/data/NUTS_RG_60M_2013.shp, accessed Oct. 2018.
[49] T. Brown, https://pypsa.org/examples/add_load_gen_trafos_to_scigrid.html, accessed Dec. 2017.
[50] U.S. Department of Energy, Electric emergency incident and disturbance report (form OE-417), https://www.oe.netl.doe.gov/OE417_annual_summary.aspx, accessed Nov. 2018.
[51] K. Purchala, L. Meeus, D. Van Dommelen, and R. Belmans, in *Proceedings of the IEEE Power Engineering Society General Meeting* (IEEE, New York, 2005), pp. 2457–2462.
[52] A. Bernstein, D. Bienstock, D. Hay, M. Uzunoglu, and G. Zussman, in *Proceedings of the IEEE Conference on Computer Communications (INFOCOM 2014), Toronto, ON* (2014), pp. 2634–2642.
[53] Z. Wang, A. Scaglione, and R. J. Thomas, IEEE Trans. Smart Grid **1**, 28 (2010).
[54] C. Matke, W. Medjroubi, and D. Kleinhans, *Mathematics and Physics of Multilayer Complex Networks, Dresden, Germany* (2015).
[55] T. Brown, J. Hörsch, and D. Schlachtberger, J. Open Res. Software **6** (2018) 4.
[56] Y. Yang, T. Nishikawa, and A. E. Motter, Science **358**, eaan3184 (2017).
[57] X. Bai, Nature (London) **559**, 7 (2018).
[58] L. Zhang, G. Zeng, D. Li, H.-J. Huang, H. E. Stanley, and S. Havlin, Proc. Natl. Acad. Sci. U.S.A. **116**, 8673 (2019).